Bioorganic & Medicinal Chemistry Letters 23 (2013) 2590–2594

Contents lists available at SciVerse ScienceDirect

Bioorganic & Medicinal Chemistry Letters

journal homepage: www.elsevier.com/locate/bmcl

Structure-based design and optimization of 2-aminothiazole-4-carboxamide as a new class of CHK1 inhibitors

Xiaohua Huang [a,*], Cliff C. Cheng [a], Thierry O. Fischmann [b], José S. Duca [b], Matthew Richards [a], Praveen K. Tadikonda [a], Panduranga Adulla Reddy [a], Lianyun Zhao [a], M. Arshad Siddiqui [a], David Parry [c], Nicole Davis [c], Wolfgang Seghezzi [c], Derek Wiswell [c], Gerald W. Shipps Jr. [a,*]

[a] Merck Research Laboratories, 320 Bent Street, Cambridge, MA 02141, United States
[b] Merck Research Laboratories, 2000 Galloping Hill Road, Kenilworth, NJ 07033, United States
[c] Merck Research Laboratories, 901 South California Avenue, Palo Alto, CA 94304, United States

ARTICLE INFO

Article history:
Received 9 January 2013
Revised 15 February 2013
Accepted 25 February 2013
Available online 7 March 2013

Keywords:
CHK1 protein kinase
2-Aminothiazole-4-carboxamide
Hybrid compounds
Structure-based drug design

ABSTRACT

Drug design efforts in the emerging 2-aminothiazole-4-carboxamide class of CHK1 inhibitors have uncovered specific combinations of key substructures within the molecule; resulting in significant improvements in cell-based activity while retaining a greater than one hundred-fold selectivity against CDK2. The X-ray crystal structure of a complex between compound **39** and the CHK1 protein detailing a 'U-shaped' topology and key interactions with the protein surface at the ATP site is also reported.

CHK1 is a serine/threonine protein kinase that arrests the cell cycle progression in response to the DNA damage induced by particular anticancer therapeutics; enabling the deployment of cellular repair mechanisms.[1] CHK1 mediates the S and G2/M arrest through the proteolysis of CDC25A[2–4] that leads to the inactivation of CDK2, whose activity is required in the cell cycle transition.[5] Coupled with the loss of the G1 checkpoint in most tumor cells due to the mutation of the tumor suppressor gene p53,[6] CHK1 downregulation abrogates additional checkpoints in the cell cycle causing tumor cells with damaged DNA to progress into catastrophic mitosis. Therefore, CHK1 inhibition should sensitize p53-defective tumor cells to the cytotoxic effects of anticancer DNA-damaging agents and lead to an expanded therapeutic window; a hypothesis that has prompted widespread attention to the discovery and development of CHK1 inhibitors over the past few years.[7–9]

In our previous account of a novel series of thiazole-4-carboxamide-based CHK1 inhibitors,[10] which were developed from the Automated Ligand Identification System (ALIS) screening hit **1**,[11] significant improvements were achieved in a biochemical CHK1 kinase inhibition assay resulting in compounds with single digit nanomolar potency. As CDK2 activity was anticipated to oppose the desired therapeutic effects of CHK1 inhibition the series was also optimized for its selectivity against CDK2 and some of the most promising compounds exhibited well above a hundred-fold selectivity. However the progression of this series was limited by weak cell-based activity, with the highest potency in low micromolar ranges assessed by the γ-H2AX cellular biomarker for DNA double-strand breaks.[12] When cancerous cells are treated with a ribonucleotide reductase inhibitor hydroxyurea (HU),[13] the checkpoint kinase CHK1 is activated to allow the cell cycle arrest and DNA repair. The addition of a CHK1 inhibitor would abrogate this mechanism and accelerate the progression of the damaged cancerous cells into mitosis, where they undergo the replication fork collapse and apoptosis, marked by the phosphorylation of histone H2AX known as γ-H2AX.

Significant improvements in cell-based activity and additional robust structure–activity relationship (SAR) development were necessary for further progression of the series. In light of the breakthrough in the biochemical potency and selectivity against CDK2 that was achieved through the modification of the 2-aryl group connected to the thiazole on the left hand side (LHS) of the molecule, continuing modification at this region with a focus on the nitrogen-linked appendage was prioritized (Table 1). These analogs were prepared following Scheme 1. The amide intermediate was prepared from 2-bromothiazole-4-carboxylic acid and the aniline using HATU as the coupling reagent. Palladium catalyzed amination of the 2-bromo intermediate using the phosphine ligand

* Corresponding authors. Tel.: +1 617 992 3174.
E-mail addresses: xiaohua.huang@merck.com (X. Huang), gshipps@comcast.net (G.W. Shipps).

0960-894X/$ - see front matter © 2013 Elsevier Ltd. All rights reserved.
http://dx.doi.org/10.1016/j.bmcl.2013.02.108

Table 1
SAR at the 2-aminothiazole position[a,b]

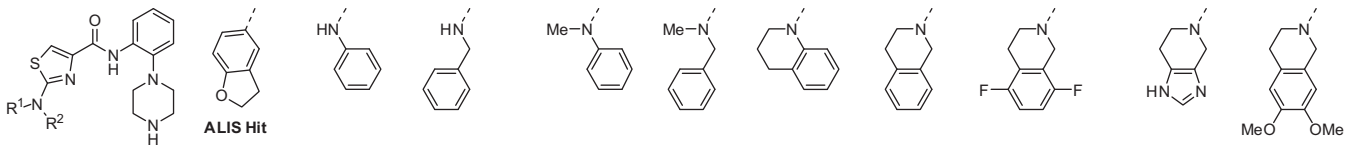

Compound #	1	2	3	4	5	6	7	8	9	10
CHK1 IC_{50} (nm)	75	92	11,000	240	>50,000	38	38	1300	4000	29
CDK2/CHK1	2.8	9	nd	19	nd	90	90	3	nd	380
H2AX EC_{50} (nm)	10000	nd	nd	nd	nd	nd	nd	nd	nd	nd

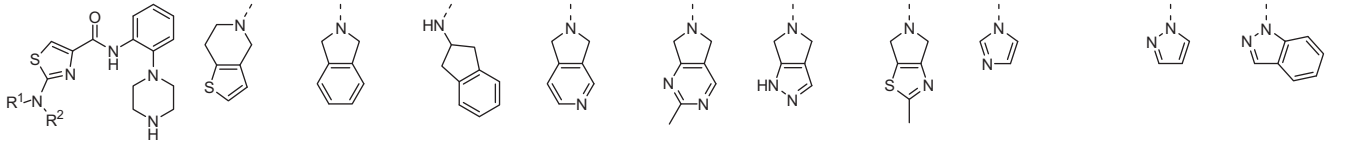

Compound #	11	12	13	14	15	16	17	18	19	20
CHK1 IC_{50} (nm)	39	8	6900	190	5700	62	280	10000	120	2
CDK2/CHK1	120	290	nd	nd	nd	nd	nd	nd	nd	500
H2AX EC_{50} (nm)	nd	1400	nd	nd	nd	nd	nd	nd	nd	750

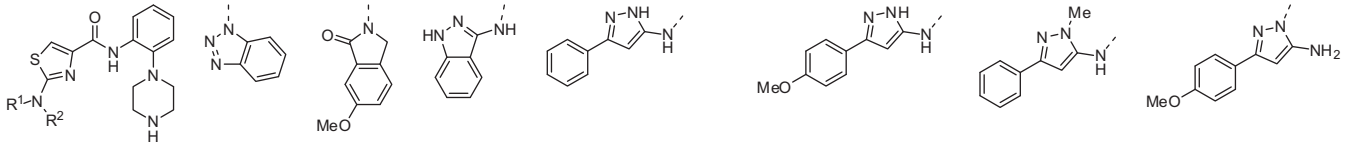

Compound #	21	22	23	24	25	26	27
CHK1 IC_{50} (nm)	110	5	2	14	3	4500	980
CDK2/CHK1	nd	4800	720	880	4300	nd	nd
H2AX EC_{50} (nm)	nd	250	350	7500	3750	nd	nd

[a] Biochemical data represent average values of duplicates or triplicates with a standard deviation of ±10%.
[b] nd, not determined.

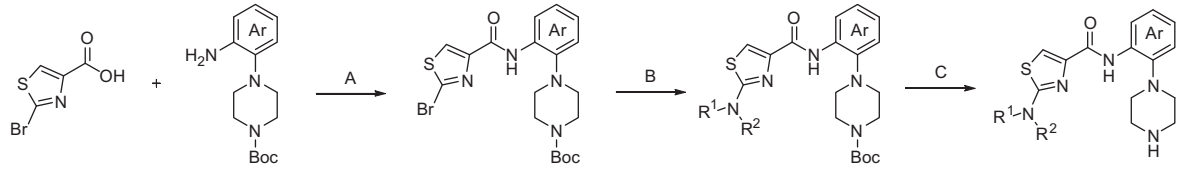

Scheme 1. Synthesis of substituted 2-aminothiazole-4-carboxamides. Reagents and conditions: (A) HATU (*N,N,N′,N′*-tetramethyl-*O*-(7-azabenzotriazol-1-yl)uronium hexafluorophosphate), DIEA (*N,N*-diisopropylethylamine), DMF, rt; (B) $Pd_2(DBA)_3$, Xantphos (4,5-bis(diphenylphosphino)-9,9-dimethylxanthene) or X-Phos (2-dicyclohexylphosphino-2′,4′,6′-triisopropylbiphenyl), HNR^1R^2, Cs_2CO_3, dioxane, 100 °C; (C) TFA (trifluoroacetic acid).

Xantphos[14] or X-Phos[15] afforded the substituted 2-aminothiazole derivatives. The removal of the Boc protecting group on the right hand side of the compounds using TFA gave the final products.

Elaboration of the 2-thiazole position was guided by both ligand and structure-based design considerations. An array of amines with steric and electronic variations were linked to the 2-thiazole. The substitution with aniline provided compound **2** with the IC_{50} of 92 nM and the selectivity against CDK2 of ninefold. Elongation to benzylamino (**3**) resulted in the significant potency decrease to 11,000 nM. Capping the aniline or benzyl amine with a methyl group (**4** or **5**) also proved to weaker relative to **1**. In light of the preferred substructure at the 2-thiazole position, the fused bicyclic aromatics that were reported in the previous account,[10] we were particularly interested in their N-containing isosteres, tetrahydroquinolines and indoline analogs. Interestingly, substitution with tetrahydroquinolinyl (**6**) and tetrahydroisoquinolinyl (**7**) demonstrated improvements in potency to less than 50 nM and selectivity against CDK2 to 90-fold. Modification of the phenyl ring in the tetrahydroisoquinolinyl proved to be quite sensitive in affecting the potency and selectivity against CDK2. While substitution with electron-withdrawing atom fluorine at the 4- and 7-positions (**8**) or changing the phenyl ring to imidazole (**9**) led to a decrease in potency to IC_{50}'s in the micromolar range, substitution with the electron donating group methoxy at the 5- and 6-positions (**10**) or changing the phenyl ring to a thiophene (**11**) retained a potency to an IC_{50} value below 50 nM and selectivity against CDK2 over 100-fold. Changing the tetrahydroisoquinoline to an isoindoline (**12**) was rewarded with an improvement in the biochemical activity to single-digit nanomolar and selectivity against CDK2 to ~300-fold. Moving the endocyclic isoindoline nitrogen out of the ring into an exocyclic position (**13**) resulted in a much weaker CHK1 inhibitor. The change of the phenyl ring in the isoindoline to other heterocycles such as pyridine (**14**), 2-methylpyrimidine (**15**), pyrazole (**16**) and 2-methylthiazole (**17**) was accompanied by a decrease of potency ranging from double-digit nanomolar to micromolar.

One of the design principles we wanted to explore was the addition of new H-bond interactions with CHK1. An area that we targeted early on was to compliment the backbone H-bond donor of Cys87. As the 2-position of the thiazole was modified it became evident that notable differences in potency could be obtained by changing the heteroaryl groups used in this LHS position. While the imidazole analogue (**18**) was a weak inhibitor with an IC_{50} of 10 μM, pyrazole (**19**) was 100-fold more potent with an IC_{50} of

120 nM. Fused heterocycles also behaved differently in their interaction with CHK1 protein. The use of indazole (**20**) on the LHS markedly improved the biochemical potency to 2 nM and the cell-based activity to 750 nM with a 500-fold selectivity against CDK2; consistent with a possible new interaction between the lone pair of the indazole nitrogen and the Cys87 amide. The benzotriazole analog (**21**) was less active with an IC_{50} of 110 nM; possibly due its weaker ability to accept an H-bond from the Cys87 and/or repulsive interactions with the additional triazole nitrogen and a nearby protein carbonyl group. Substitution with 6-methoxyisoindolinone (**22**) or 3-aminoindazole via the primary amino group (**23**) provided compounds with the biochemical activity in the same range as compound **20**, but was about threefold more active in the cell assay with better selectivity against CDK2. 3-Aryl-5-aminopyrazole derivatives were also examined. The 3-phenyl-5-aminopyrazole analog (**24**) suffered from poor cellular potency despite its active inhibition of CHK1 kinase activity. *para*-Methoxyl substitution to 3-phenyl group (**25**) that fit well in the solvent exposed region improved the potency by several fold,[16] but remained above 1 μM in cells. Adding a methyl group (**26**) or moving the connection (**27**) to the pyrazolyl nitrogen brought down the enzymatic potency drastically to the micromolar range, possibly due to the disruption of interactions with the H-bond donor on the Cys87 residue by the methyl group (**26**) or exocyclic NH functionality (**27**), and/or an unfavorable orientation of the distal phenyl ring.

To establish additional SAR trends, a scan of different isomeric pyridines was performed on the phenyl ring of the right hand side (RHS) of the molecule (Table 2). With the possibility of gaining an additional H-bond interaction between a pyridine ring nitrogen and the catalytic Lys38, we prioritized the synthesis of compound **30**. A slight improvement in the biochemical potency and selectivity against CDK2 in the pyridine analog with a *para*-piperazine substitution (**30**) was also obtained; the other 3 isomeric pyridines (**28**, **29**, and **31**) suffered from potency losses ranging from a few fold to over tenfold relative to compound **1** as they may not place the pyridyl nitrogen in an optimal position to H-bond to Lys38. A loss of selectivity against CDK2 in compound **29** was also evident, presumably because the side-chain homologous CDK2 Lys33 shows extended flexibility and more readily accommodates a less favorable orientation of the pyridinyl H-bond acceptor compared to CHK1.[17] Consequently, additional compounds with the same RHS as **30** were prepared incorporating other favorable groups on the LHS identified from both the previous account, such as 5-benzofuran (**32**), 5-indole (**33**), 5- and 2-benzothiophene (**34** and **35**), and others detailed in Table 1 of this article (see Table 3). In the class of 2-aryl thiazoles cell-based activity still remained in the micromolar range, and in the case of *para*-phenoxy phenyl substitution (**36**), a significant drop in the biochemical activity was also observed. Interestingly, the 2-amino substituent appended to the thiazole on the LHS and the pyridine on the RHS demonstrated a combined favorable influence on the cell-based activity, and pronounced improvement to an EC_{50} of 30 nM in the best case (**39**) was observed (see the Supplementary data for the activity assessment in the presence and absence of hydroxyurea). The *des*-OMe analog (**38**) is threefold less potent in H2AX cell-based assay. While the combination of isoindoline on the LHS and pyridine on the RHS (**37**) did not gain much in terms of cell-based activity, the hybrids with indazole (**40**) or 3-aminoindazole (**41**) on the LHS gave a 10-fold potency boost in the cell-based assay to 75 and 40 nM respectively, relative to the analogs with the same LHS group in Table 1 (**20** and **23**).

To elucidate the binding mode of this new class of CHK1 inhibitors with the protein, the X-ray crystal structure of the complex between compound **39** and the CHK1 protein at a resolution of 1.70 Å was successfully obtained (Fig. 1).[18] Many of key interactions observed between compound **1** and CHK1 were retained in the binding of compound **39**.[10] Intramolecular H-bonds amongst the secondary amide, tertiary anilinic *N* and the thiazolyl *N* stabilize a 'U-shaped' topology to **39**. The salt bridge between the distal piperazinyl NH and Glu91 and Glu134 and H-bond between the carbonyl O of the amide and conserved water are identical to the previously reported X-ray.[10] A slight difference in the hinge interaction is observed including the attraction between carbonyl *O* in Glu85 and thiazolyl *S*.[19] In agreement with the initial hypothesis a new H-bond between Cys87 NH and the carbonyl *O* of the isoindolinone group is evident. In addition, the design efforts on the RHS of the compound yielded another hydrogen bond between the pyridinyl *N* and the Lys38. To further probe this H-bond interaction, modifications in the vicinity of the pyridinyl *N* were made (Table 4). The replacement of pyridine with fluorobenzene (**42**) retained the biochemical potency in the single-digit nanomolar range and excellent selectivity against CDK2, suggesting the

Table 2
Replacement of phenyl ring with pyridines on the RHS of the molecule[a,b]

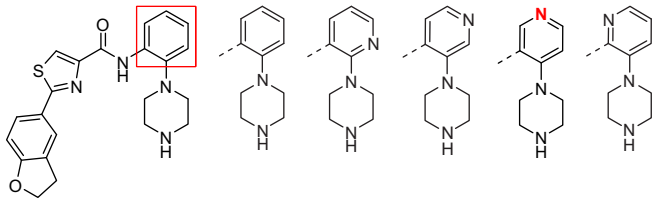

Compound #	**1**	**28**	**29**	**30**	**31**
CHK1 IC_{50} (nm)	75	870	230	55	4700
CDK2/CHK1	2.8	nd	0.11	8.2	3

[a] Biochemical data represent average values of duplicates or triplicates with a standard deviation of ±10%.
[b] nd, not determined.

Table 3
Hybrid compounds[a,b]

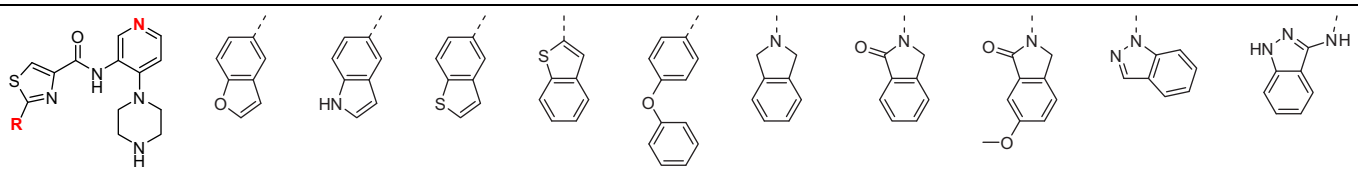

Compound #	**32**	**33**	**34**	**35**	**36**	**37**	**38**	**39**	**40**	**41**
CHK1 IC_{50} (nm)	28	10	7	3	430	8	2	1	3	3
CDK2/CHK1	nd	430	210	65	nd	130	2580	11000	100	550
H2AX EC_{50} (nm)	nd	1000	1250	1000	nd	900	100	30	75	40

[a] Biochemical data represent average values of duplicates or triplicates with a standard deviation of ±10%.
[b] nd, not determined.

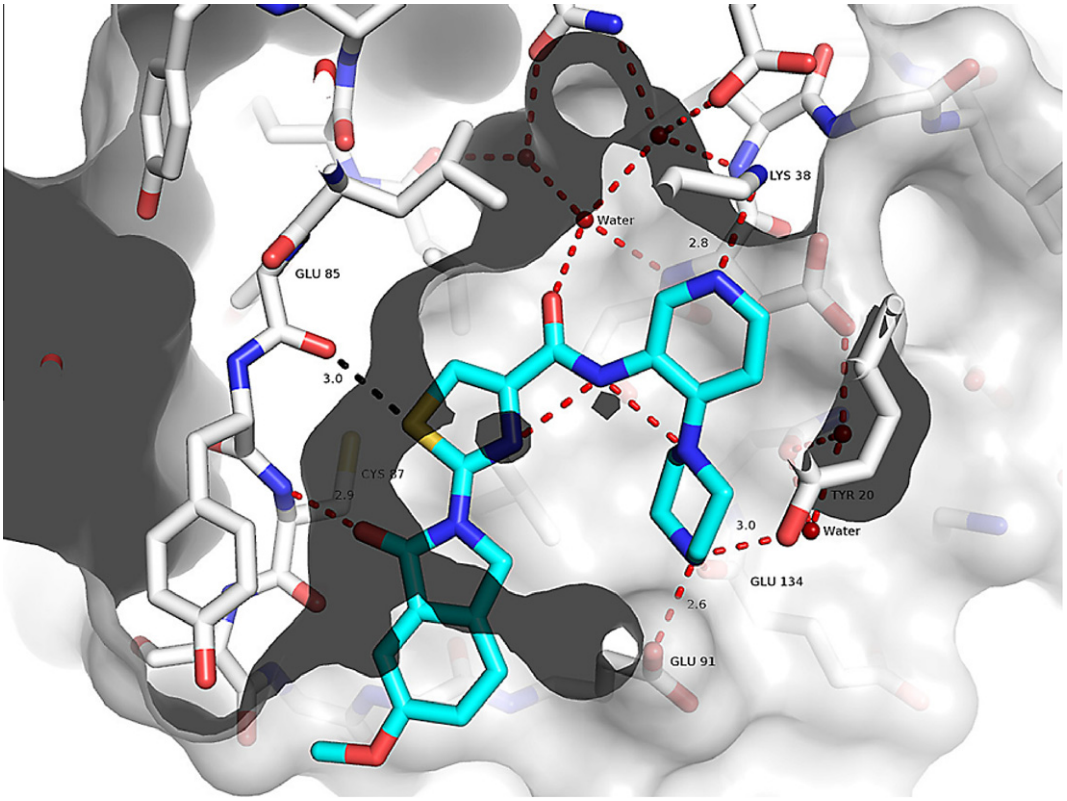

Figure 1. X-ray of crystal structure of compound **39** bound to CHK1 protein.

Table 4
Optimization to Probe Interaction with Lys38 [a,b]

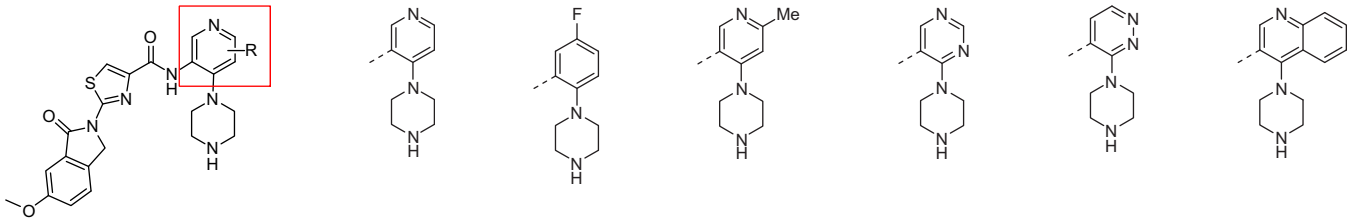

Compound #	**39**	**42**	**43**	**44**	**45**	**46**
CHK1 IC_{50} (nm)	1	4	10	46	281	5200
CDK2/CHK1	11,000	10,000	5000	nd	nd	nd
H2AX EC_{50} (nm)	30	6000	1000	nd	nd	nd

[a] Biochemical data represent average values of duplicates or triplicates with a standard deviation of ±10%.
[b] nd, not determined.

charge-dipole or H-bond interaction between C–F bond and Lys38.[20] The large loss in cellular potency to 6 μM might be due to the confounding off-target effect or efflux from the cell. Adding a methyl group next to the pyridinyl *N* (**43**) or changing the pyridine to pyrimidine (**44**), pyridazine (**45**) or quinoline (**46**) imparted a reduction in biochemical activity from tenfold to several thousand folds due to unfavorable steric or electronic interactions.

Compound **39** was further profiled for the in-house kinase selectivity, GPCR counter screening, drug interaction and hERG inhibition (see the Supplementary data). Good selectivity against an in-house kinase panel and a clean profile in GPCR counter screening were demonstrated. The good kinase selectivity might be partially explained by the salt bridge interaction with Glu91 which shows some variability among kinases. Compound **39** demonstrated no inhibition against a panel of cytochrome P450 (CYP) enzymes up to 30 μM. The cardiovascular liability was assessed using human ether-a-go-go-related gene (hERG) rubidium efflux (65% inhibition @ 5 μg/mL), IonWorks (42% inhibition @ 10 μM), and voltage clamp (82% inhibition @ 1 μM), and hERG blockade was seen in compound **39**, most likely caused by the basic piperazine. The bioavailability of compound **39** was determined in an oral rat PK experiment, where an AUC of 7.2 μM h was determined after a 10 mg/kg single dose.

In summary, drug design efforts have led to the discovery of 2-aminothiazole-4-carboxamide as a new class of CHK1 inhibitors that are potent in both enzymatic and cell-based assays with over a hundred fold selectivity against CDK2. The overall profile of this novel series of CHK1 inhibitors represented by compound **39** provided a solid base for further optimization efforts towards a potential clinical candidate as will be reported at a later date.

Acknowledgments

We thank all legacy Schering-Plough colleagues who contributed in many meaningful ways to initiating and sustaining the hit to lead and lead optimization of the thiazole-4-carboxamide-based CHK1 inhibitor project and all supporting management, including Timothy J. Guzi, Satish Jindal, Neng-Yang Shih and John J. Piwinski.

Supplementary data

Supplementary data associated with this article can be found, in the online version, at http://dx.doi.org/10.1016/j.bmcl.2013.02.108.

References and notes

1. Tapia-Alveal, C.; Calonge, T. M.; O'Connell, M. J. *Cell Div.* **2009**, 4.
2. Mailand, N.; Falck, J.; Lukas, C.; Syljuåsen, R. G.; Welcker, M.; Bartek, J.; Lukas, J. *Science* **2000**, *288*, 1425.
3. Xiao, Z.; Chen, Z.; Gunasekera, A. H.; Sowin, T. J.; Rosenberg, S. H.; Fesik, S.; Zhang, H. *J. Biol. Chem.* **2003**, *278*, 21767.
4. Xiao, Z.; Xue, J.; Sowin, T. J.; Rosenberg, S. H.; Zhang, H. *Oncogene* **2005**, *24*, 1403.
5. Guadagno, T. M.; Newport, J. W. *Cell* **1996**, *84*, 73.
6. Levine, A. J. *Cell* **1997**, *88*, 323.
7. Ma, C. X.; Janetka, J. W.; Piwnica-Worms, H. *Trends Mol. Med.* **2011**, *17*, 88.
8. Garrett, M. D.; Collins, I. *Trends Pharmacol. Sci.* **2011**, *32*, 308.
9. (a) Oza, V.; Ashwell, S.; Almeida, L.; Brassil, P.; Breed, J.; Deng, C.; Gero, T.; Grondine, M.; Horn, C.; Ioannidis, S.; Liu, D.; Lyne, P.; Newcombe, N.; Pass, M.; Read, J.; Ready, S.; Rowsell, S.; Su, M.; Toader, D.; Vasbinder, M.; Yu, D.; Yu, Y.; Xue, Y.; Zabludoff, S.; Janetka, J. *J. Med. Chem.* **2012**, *55*, 5130; (b) Montano, R.; Chung, I.; Garner, K. M.; Parry, D.; Eastman, A. *Mol. Cancer Ther.* **2012**, *11*, 427.
10. Huang, X.; Cheng, C. C.; Fischmann, T. O.; Duca, J. S.; Yang, X.; Richards, M.; Shipps, G. W., Jr. *ACS Med. Chem. Lett.* **2012**, *3*, 123.
11. Annis, A.; Chuang, C.-C.; Nazef, N. ALIS: An Affinity Selection-Mass Spectrometry System for the Discovery and Characterization of Protein-Ligand Interactions. In *Methods and Principles in Medicinal Chemistry*; Wanner, K., Höfner, G., Eds.; Mass Spectrometry in Medicinal Chemistry: Applications in Drug Discovery; Mannhold, R., Kubinyi, H., Folkers, G., Eds.; Wiley-VCH: Weinheim, 2007; Vol. 36, Chapter 3.
12. Rogakou, E. P.; Pilch, D. R.; Orr, A. H.; Ivanova, V. S.; Bonner, W. M. *J. Biol. Chem.* **1998**, *273*, 5858.
13. Elford, H. L. *Biochem. Biophys. Res. Commun.* **1968**, *33*, 129.
14. Yin, J.; Zhao, M. M.; Huffman, M. A.; McNamara, J. M. *Org. Lett.* **2002**, *4*, 3481.
15. Anderson, K. W.; Tundel, R. E.; Ikawa, T.; Altman, R. A.; Buchwald, S. L. *Angew. Chem., Int. Ed.* **2006**, *45*, 6523.
16. Caldwell, J. J.; Welsh, E. J.; Matijssen, C.; Anderson, V. E.; Antoni, L.; Boxall, K.; Urban, F.; Hayes, A.; Raynaud, F. I.; Rigoreau, L. J. M.; Raynham, T.; Aherne, G. W.; Pearl, L. H.; Oliver, A. W.; Garrett, M. D.; Collins, I. *J. Med. Chem.* **2011**, *54*, 580.
17. Fischmann, T. O.; Hruza, A.; Duca, J. S.; Ramanathan, L.; Mayhood, T.; Windsor, W. T.; Le, H. V.; Guzi, T. J.; Dwyer, M. P.; Paruch, K.; Doll, R. J.; Lees, E.; Parry, D.; Seghezzi, W.; Madison, V. *Biopolymers* **2008**, *89*, 372.
18. The atomic coordinates of compound **39** bound to CHK1 have been deposited in the Protein Data Bank: PDB ID, 4HYH.
19. Lu, J.; Lu, Y.; Yang, S.; Zhu, W. *Struct. Chem.* **2011**, *22*, 757.
20. (a) Müller, K.; Faeh, C.; Diederich, F. *Science* **2007**, *317*, 1881; (b) Razgulin, A. V.; Mecozzi, S. *J. Med. Chem.* **2006**, *49*, 7902.